Lasers in Manufacturing Conference 2021

Laser polishing of laser micro weld seams on Cu-ETP and CuSn6 with green laser radiation

Moritz Küpper[a,*], Marc Hummel[a], Rakesh Kumar Pandey [b], Constantin Häfner[a]

[a]*Chair for Laser Technology (LLT), RWTH Aachen University, Steinbachstr. 15, Aachen 52074, Germany*
[b]*Material Science and Nanotechnology, Politecnico di Milano, Piazza Leonardo da Vinci 32, Milano, Italy*

Abstract

Copper and copper alloys used in electrical applications can be contacted by laser micro welding. The achievable roughness of these micro weld seams can be too large for some applications (like sealing surfaces or to minimize surface oxidation). Up to now laser polishing, which smoothens the surface due to surface tension in the molten state, of copper could not be demonstrated successfully with industry common infrared high power laser systems typically used for laser polishing. This study investigates the use of green 515 nm wavelength high power laser sources for laser polishing of pure copper (Cu-ETP) and a widely used copper alloy (CuSn6). A suitable process window is identified by variation of process parameters (laser beam diameter, scanning speed, laser power) for single and overlapping remelting tracks. The best parameters are tested on laser micro weld seams created with the same setup to smoothen their rough surface.

Keywords: laser polishing; laser micro welding; copper; CuSn6; green laser radiation

1. Introduction

Copper and copper alloys are widely used in electrical applications due to their good electrical and thermal conductivity. Laser micro welding is used to precisely join small and thin copper parts found for example in batteries and electronics for e-mobility as described by Schmidt, 2015. The surface of these micro weld seams often is relatively rough due to fluctuations in the melt pool and keyhole caused for example by inhomogeneities in the material. For some applications (like sealing surfaces or to minimize surface oxidation) a smoother surface is favorable. Laser polishing remelts the metal surface and uses the surface

* Corresponding author. Tel.: +49 241 8906 299; fax: +49 241 8906 121.
E-mail address: moritz.kuepper@llt.rwth-aachen.de

tension of the melt to redistribute material, thereby smoothening the surface as investigated by Willenborg 2006 on tool steel. Up to now, laser polishing of copper has not been demonstrated successfully.

This is mainly due to the infrared wavelength of the laser radiation in the range of 1030 to 1080 nm of most industry common high power laser systems typically used for laser polishing. Copper absorbs only a few percent of this wavelength in the solid state while absorbing significantly more in the molten state [Hummel et al. 2020]. This makes it difficult to create a stable melt pool as it is required for laser polishing. Laser welding on the other hand is already possible with infrared laser radiation as it uses much higher laser intensities to evaporate the material and form a keyhole to enable deep welding. This study investigates the use of newly available high power laser sources with green laser radiation (515 nm) which shows much higher absorptivity in copper and copper alloys (see Fig. 1. (a)) and therefore has the potential to enable laser polishing. The experiments are carried out on pure copper (Cu-ETP) and a widely used copper alloy (CuSn6). Their most important difference with respect to laser processes is their large difference in heat conductivity (Cu-ETP: 390 W/m*K vs. CuSn6: 75 W/m*K)).

2. Objectives and methodology

No previous work on laser polishing of copper with green laser radiation is documented. Therefore in the first step experiments comprise the variation of process parameters (laser beam diameter, scanning speed, laser power) for single remelting tracks. Two different laser beam diameters (100 µm and 220 µm) as well as three different scanning speeds (50; 100 and 200 mm/s) are investigated. The laser power is increased from minimum (120 W) up to the point were obvious evaporation by plasma formation is observed.
The objective is, to investigate differences in laser remelting of Cu-ETP and CuSn6 by measuring the track width and identify process parameter ranges for stable remelting, as is required for laser polishing. This also allows to narrow down the process window for polishing an area by overlapping remelting tracks in the second step of experiments. The roughness of the areal polished test fields is measured using a white light interferometer (Zygo NewView 7300). These first two steps are carried out on 1 mm thick sample sheets.
Finally in the third step the best process parameters identified are tested on laser micro weld seams created with the same setup to smoothen their rough surface. Here samples of 3 mm thickness are used.
Additionally to the effect of laser power and scanning velocity, different number of polishing passes and scanning strategies are investigated. The resulting topography and roughness are measured using optical microscopy (Keyence VHX 6000). Also etched metallographic cross sections (using etching agents V2A for Cu-ETP and Adler 2:1 for CuSn6) are created to examine remelt depth and quality.

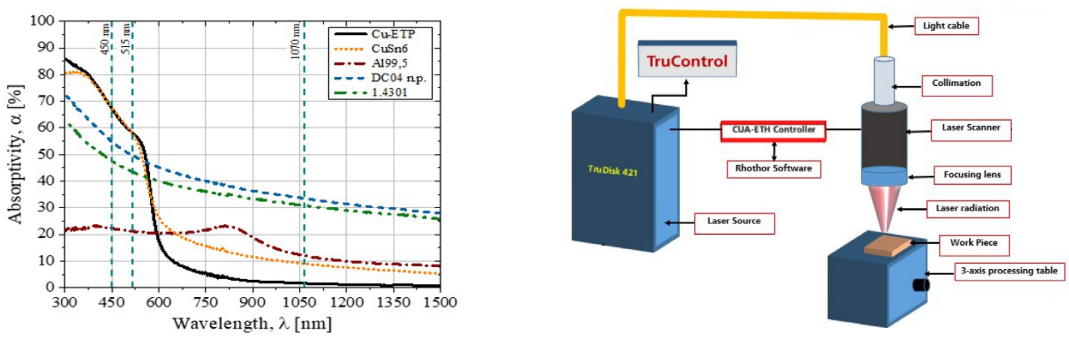

Fig. 1. (a) Comparison graph of absorptivity with 1070 nm,515 nm,and 450 nm wavelength for Cu-ETP and CuSn6 [Hummel et al. 2020]
(b) Schematic representation of experimental set-up of TRUMPF TruDisk Pulse 421 with beam shaping and deflection system.

All experiments are carried out under normal atmosphere. Usually a shielding gas like argon is used for laser polishing, to prevent oxidation in the melt. This is chosen to investigate the practicability of a simultaneous or consecutive laser polishing of weld seams directly on the laser welding machine, which typically operates under normal atmosphere.

3. Experimental setup

As green laser source a Trumpf TruDisk Pulse 421 with a laser wavelength of 515 nm is used. Its maximum pulse length of 50 ms is used with single rectangular pulses to mimic cw laser radiation (typically used for laser polishing) as close as possible. It allows laser powers of 120 W to 1000 W for this pulse type. A Typical 2D-Scanner setup was used in which the laser radiation is guided through a light cable, collimated into a 2D-Newson Scanner (2D-MSA-A20) and focused through a f-Theta objective onto the sample surface, as depicted in figure 1b. Two different focusing lenses allowed laser beam diameters of 100 µm and 220 µm with a top-hat intensity profile. High reflective coatings on mirrors and anti reflective coatings on lenses are specified for the green laser radiation wavelength of 515 nm. Scanner and laser source are controlled by the control card (CUA-ETH) and Rothor Software from Newson.

4. Results and discussion

4.1. Investigations on single melt tracks

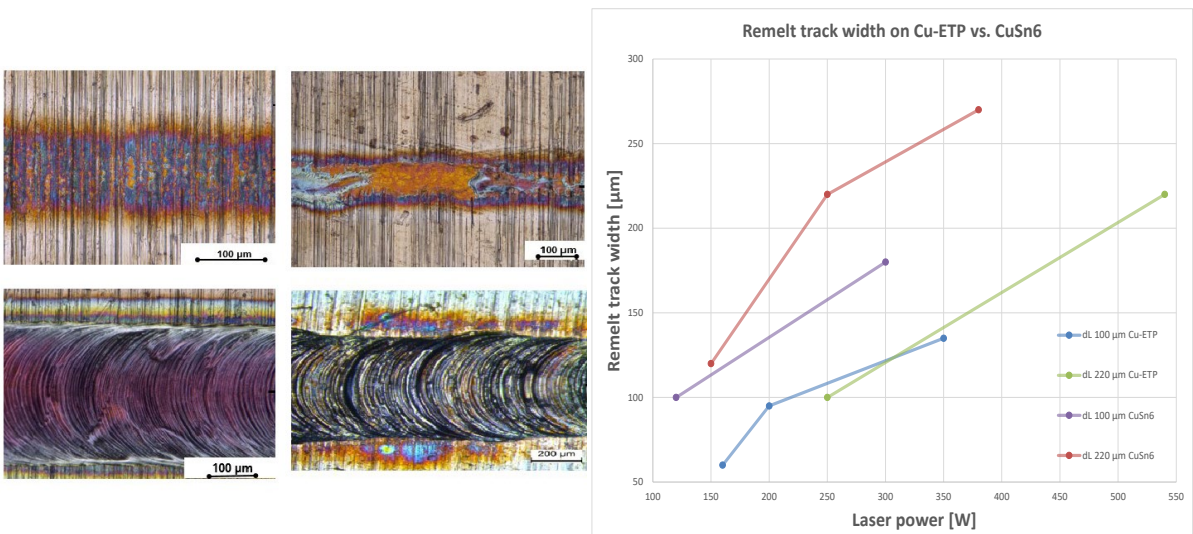

Fig. 2. (a) Microscopic images of examples of laser remelt tracks on Cu-ETP. From no remelting (top left), unstable remelting (top right) and stable remelting (bottom left) to fluctuating remelting with plasma (bottom right);
(b) Comparison graph of track width over laser power for both beam diameters and materials investigated (each graph combines results for three scanning velocities).

Examples of the different types of observed remelt tracks on Cu-ETP are depicted in Fig. 2.(a). Cu-ETP displays vivid tempering colors due to oxidation, which are not observed on CuSn6. Although a slight trend towards narrower tracks width with higher scanning velocity is observable, the track widths varied only little

for the three scanning speeds within the range of error on both materials. Therefore for comparison, the measured tracks widths for the three scanning velocities are combined into one graph each for the two laser beam diameters and materials in Fig. 2. (b). Each graph starts at the lowest laser power, at which stable melting was observed and ends with the laser power at which first plasma was observed. Several conclusions can be drawn from this comparison.

Melted track width at same laser power achieved in material CuSn6 is always higher than on Cu-ETP with both laser beam diameters. Also the respective minimum and maximum laser powers are significantly lower on CuSn6 compared to Cu-ETP. In general for Cu-ETP the graphs are shifted towards lower track sizes and higher laser powers. The maximum achievable track widths are higher for CuSn6 compared to Cu-ETP with both beam diameters. Since the melting points are relatively similar (Cu-ETP 1083 °C vs. CuSn6 1040 °C) this could be caused by different absorptions of the laser energy but is probably best explained by the large difference in thermal conductivity between the two materials. Pure copper CU-ETP conducts heat approx. 5 times better than CuSn6. This means that on Cu-ETP more of the laser energy absorbed on the surface is quickly dissipated into the bulk of the material while on CuSn6 more of this energy is longer concentrated at the surface, where it leads to the formation of larger melt pools with higher temperatures. This can only partially be compensated with higher laser power. The increased intensities necessary to achieve the same track width on Cu-ETP cause melt pool surface temperatures to rise above the evaporation temperature and therefore create plasma before the same maximum track width compared to CuSn6 can be reached.

Laser beam diameter 220 µm on CuSn6 and laser beam diameter 100 µm on Cu-ETP show a change in slope in the graph. The change in slope is observed, when melting track width reaches the laser beam diameter i.e., 220 µm for CuSn6 and 100 µm for Cu-ETP. The decrease in slope means, that the melt pool grows slower with increasing laser power. This is due to the fact that once the track width reaches the laser spot size it can only grow further due to heat conduction in the material. Below this limit it grows faster with laser power because the surface under the laser spot is mainly heated by absorbing the laser radiation and only a small portion originates from the heat conduction of the already molten material in the middle of the laser spot. Laser beam diameter 220 µm on Cu-ETP and laser beam diameter 100 µm on CuSn6 do not show a change in slope, instead the graph increases linearly for both cases. Laser beam diameter 100 µm on CuSn6 achieved a melting track width of 100 µm equal to the laser beam diameter at minimum available laser power of 120 W. It is expected that the graph would continue downwards with greater slope for lower laser powers. This should be investigated in future works using an attenuator or a different laser source. In the case of laser beam diameter of 220 µm on Cu-ETP, plasma started after reaching the melting track width similar to the laser beam diameter. Therefore the regime of slower melt pool growth beyond this point does not occur in this case.

4.2. Areal polishing

To laser polish an area, several re-melting tracks are offset below each other with a track offset *dy*, smaller than the width of a single re-melting track. In these experiments a fixed track offset of 30 µm is chosen for the laser beam diameter d_L = 100 µm and *dy* = 50 µm for the laser beam diameter d_L = 220 µm. These values are about one-fourth of the average remelt track width for the respective laser spot size discovered in the single track experiments. Therefore the surface is re-melted three to five times, depending on the laser power. This is a typical overlap for laser polishing as used by Willenborg 2006.

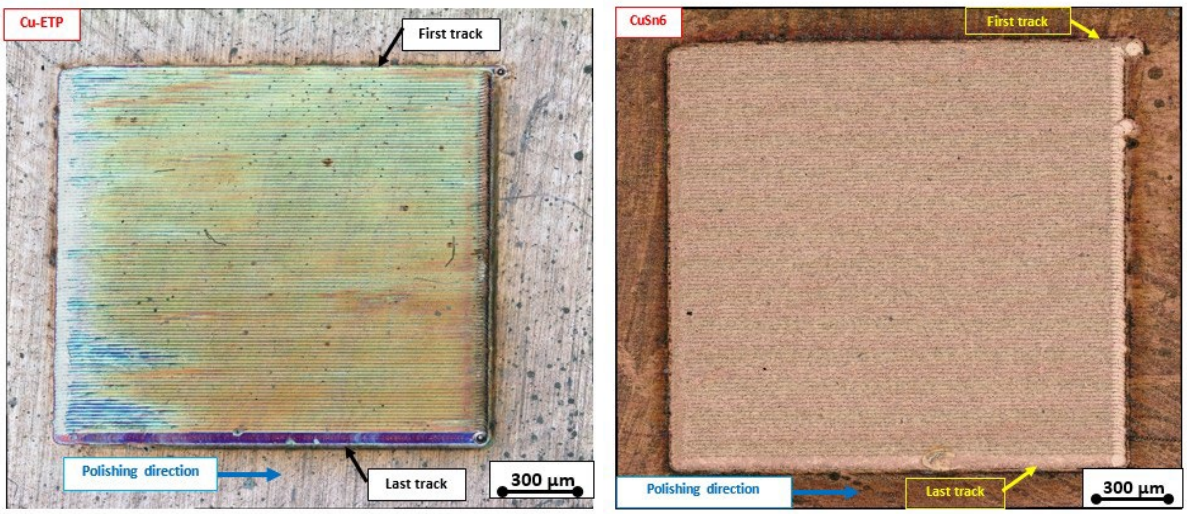

Fig. 3. (a) Microscopic image of "best" laser polished area on Cu-ETP. Visible tempering colors due to oxidation.
(b) Microscopic image of "best" laser polished area on CuSn6. No visible tempering colors.

Stable areal laser polishing with this set-up already starts with the minimum laser power of 120 W for three combinations of laser beam diameter and material, except on Cu-ETP with the laser beam diameter of 220 µm it starts from a laser power of 180 W. Due to the lower thermal conductivity of CuSn6 a process window could not be identified for the laser beam diameter of 100 µm because the minimum laser power of 120 W was enough to evaporate the material and cause plasma.

Table 1. Comparison of obtained minimum and maximum laser power range P_L for stable single melting tracks and stable area polishing for scan velocity v_s = 100 mm/s (* 120W is the available minimum laser power due to technical limitation of this set-up).

Combination of laser beam diameter and material	Single melting tracks: P_L range [W]	Areal laser polishing: P_L range [W]
d_L = 220 µm on Cu-ETP	250 - 560	200 - 300
d_L = 220 µm on CuSn6	170 - 390	120 - 220
d_L = 100 µm on Cu-ETP	150 - 350	120 - 160
d_L = 100 µm on CuSn6	*< 120 – 310	*< 120

Comparing the obtained parameters from single melting tracks and areal laser polishing in Table 1, it can be seen that in general minimum and maximum laser power are both lower in areal polishing due to the effect of pre-heating from previous re-melt tracks, as is typically observed in laser polishing of metals.
The arithmetic average areal roughness Sa is calculated from the white light interferometer measurements on the laser polished test fields and the initial state. The initial surfaces of the two materials are comparable and relatively smooth ($Sa_{initial,\ Cu\text{-}ETP}$ = 0,3 ± 0,02 µm and $Sa_{initial,\ CuSn6}$ = 0,3 ± 0,1 µm). A laser polishing parameter improving on this already smooth surface could not be identified. The best results on Cu-ETP only matched the initial roughness of Sa = 0,3 ± 0,1 µm (displayed in figure 3(a)) while other parameters increased it up to 1 µm. On CuSn6 the best result (displayed in figure 3(b)) only achieved Sa = 0,6 ± 0,1 µm (others up

to 1,6 µm), effectively increasing the initial roughness. In future work it should be investigated whether better laser polishing results can be achieved using shielding gas. The fact, that on Cu-ETP, lower roughnesses close to the initial roughness could be achieved compared to CuSn6, might be explained by the bulging of re-melted tracks observed on CuSn6 in the next section.

4.3. Laser polishing on laser micro weld seams

One result of the previous experiments is that the minimum laser power of the used laser source in combination with the smaller laser beam diameter of 100 µm creates too high intensities for the two materials investigated here. Therefore only the larger beam diameter of 220 µm is used in this step. The other parameters are varied again to determine their influence on the polishing process on this new initial surface with much higher initial roughness. To be able to target the weld seam accurately with the laser scanning system for the following laser polishing step, the welding is executed with the same experimental set-up including focusing lens and sample position. Therefore both processes are carried out with the laser beam diameter of 220 µm. For the laser micro welding the fixed process parameters chosen are: laser power P_L = 1000 W, scanning velocity v_s = 200 mm/s, single track.

The approach is to overlay a smaller laser polishing field wider than the weld seam width on top of a longer laser micro weld seam, as depicted in Fig. 4. This is chosen for two reasons. Firstly to redistribute the uneven surface of the weld seam over a larger area, thus potentially improving the polishing result. Secondly the fluctuating nature of the key hole welding process occasionally produces splatter particles that deposit next to the weld track. The chosen overlap of a few 100 µm also re-melts and smoothens these particles. To account for the fluctuating nature of the weld seam surface the roughness measurement on Cu-ETP and CuSn6 for laser weld seams and laser polishing are taken by measuring and averaging the Ra value of three parallel profile lines next to each other in the center of the track.

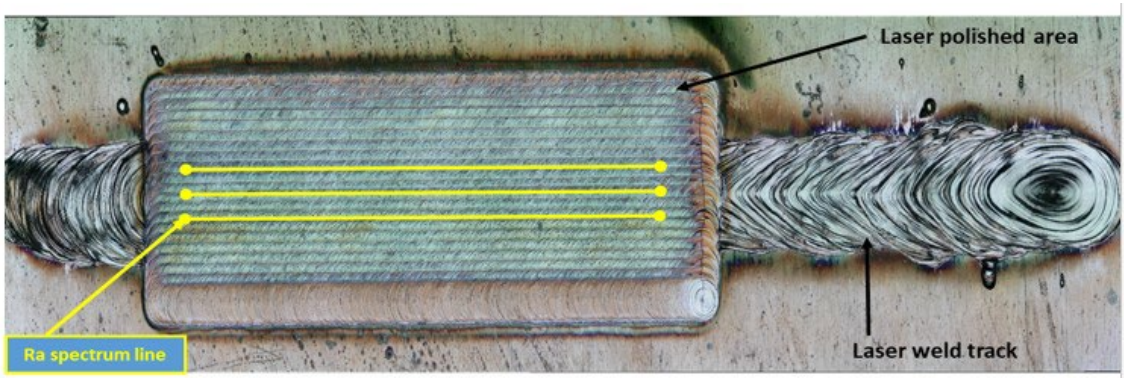

Fig. 4. Microscopic example image of a partially laser polished laser micro weld seam. Yellow lines indicate where roughness profile is measured.

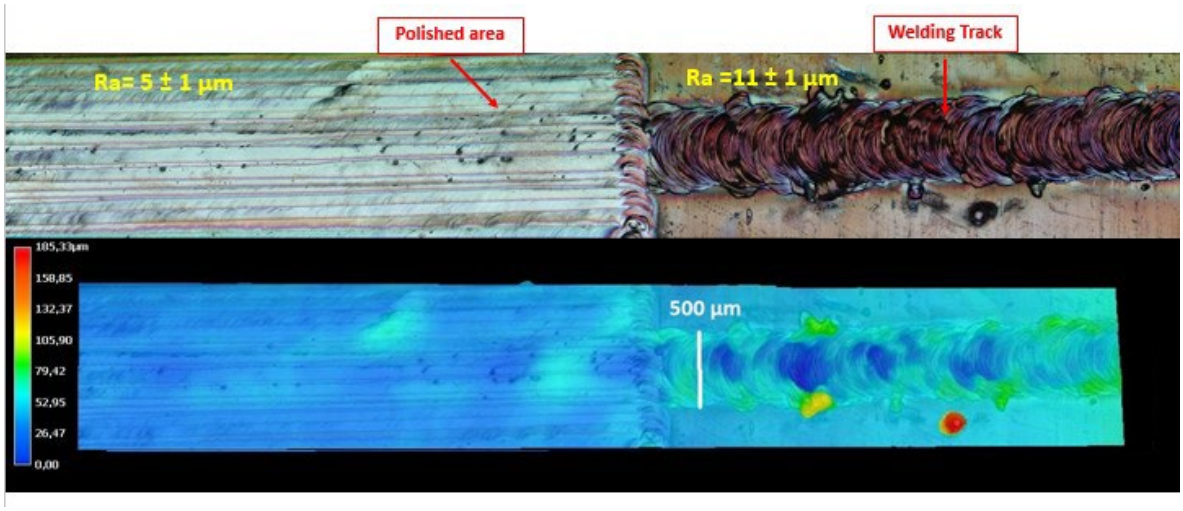

Fig. 5. (a) Microscopic image and (b) false color 3D height map of the best achieved polishing result on Cu-ETP. Polished area is smooth and local splatter particles and spikes are removed.

In this part, one new parameter number of passes `n´ (number of times of polishing) is added to improve the smoothness and quality of weld seams. Single polishing passes did not show significant smoothing in measured roughness. Therefore only higher numbers of passes where investigated (n = 2, 3, 4 passes) with scanning velocities (50; 100; 200 mm/s). In addition to investigating the influence of higher numbers of passes, three different scanning strategies where also examined. Polishing in X (0°) direction means parallel to the direction of laser micro welding. Y (90°)-polishing direction means perpendicular to the laser micro welding. Finally the combination of those two was tested, i.e. X (0°) + Y (90°)-polishing direction means first pass of polishing in parallel to welding direction then second pass of polishing perpendicular to welding direction (combination of X-Y counted as two passes and combination of X-Y + X-Y counted as 4 passes). This last strategy is often used in laser polishing to achieve good polishing results independent from dominating structure orientations as stated by Willenborg, 2006.

Results on Cu-ETP:

The track width of laser welding on Cu-ETP is 500 µm. Mean arithmetic roughness Ra of the laser micro weld seams on Cu-ETP is measured to be Ra = 11 ± 1 µm. Within the range of errors the results show no significant influence of more than two passes, scanning velocity or different scanning strategies. Therefore the simple scanning in X-direction along with the weld track, a medium scanning velocity of 100 mm/s and two passes are identified as suitable parameters. All results show a significant decrease in roughness with increasing laser power. Hence it can be concluded that the highest laser power close to the evaporation limit is the best choice in this case. This is also favorable as larger melt pools also re-melt deeper into the material which improves the possibility to heal cracks or pores under the surface. Fig. 5.(a) and (b) shows a microscopic image of the best polishing result on Cu-ETP and a false color height map calculated on the Keyence microscope of the same surface (process parameters P_L = 420 W, v_s = 100 mm/s, n = 2 passes yield a roughness of Ra = 5 ± 1 µm). The polished area is smooth and local spikes and valleys are flattened.

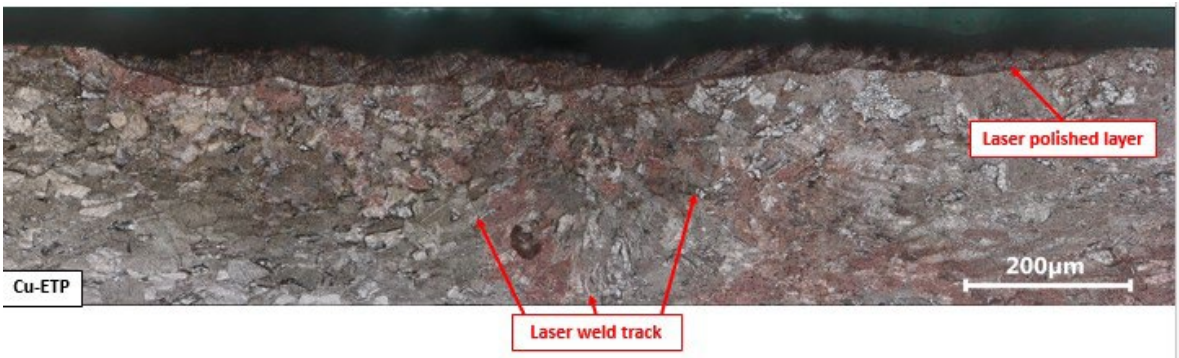

Fig. 6. Microscopic image of etched metallographic cross section of laser polished laser micro weld seam on Cu-ETP using best parameters identified. The separate laser polishing tracks are clearly visible while the contrast of the laser weld track is low and only visible in magnification. Cracks or pores are not obvious in this sample.

The cross section displayed in Fig. 6. shows a barely visible weld track. The outline of the melt pool is indicated by the arrows and is only visible under magnification. The overlapping laser polishing tracks on the other hand are clearly visible. Cracks or pores are not obvious in this sample. The depth of the laser weld track is measured with 305 ± 5 µm. The first laser polishing tracks have an average depth of 33 ± 2 µm but reach their equilibrium depth of 49 ± 2 µm after a few tracks due to the preheating effect. This shows that only about one sixth of the weld track depth is re-molten by the subsequent polishing step.

Results on CuSn6:

The track width of laser welding on CuSn6 is 640 µm. Mean arithmetic roughness Ra of the laser micro weld seams on CuSn6 is measured to be Ra = 8 ± 1 µm. The results show no significant influence of more than 2 passes, scanning velocity or different scanning directions as was discovered for Cu-ETP. Also within the range of errors similar roughnesses are achieved for medium to high laser powers.

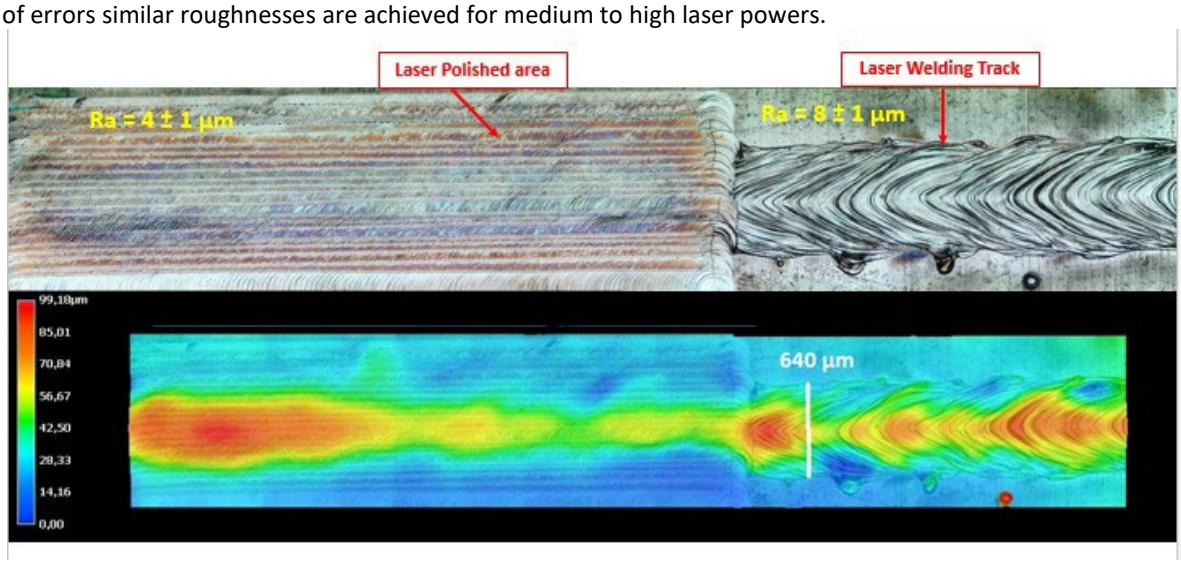

Fig. 7. (a) Microscopic image and (b) false color 3D height map of the best achieved polishing result on CuSn6. Polished area is smooth and local splatter particles and spikes are removed.

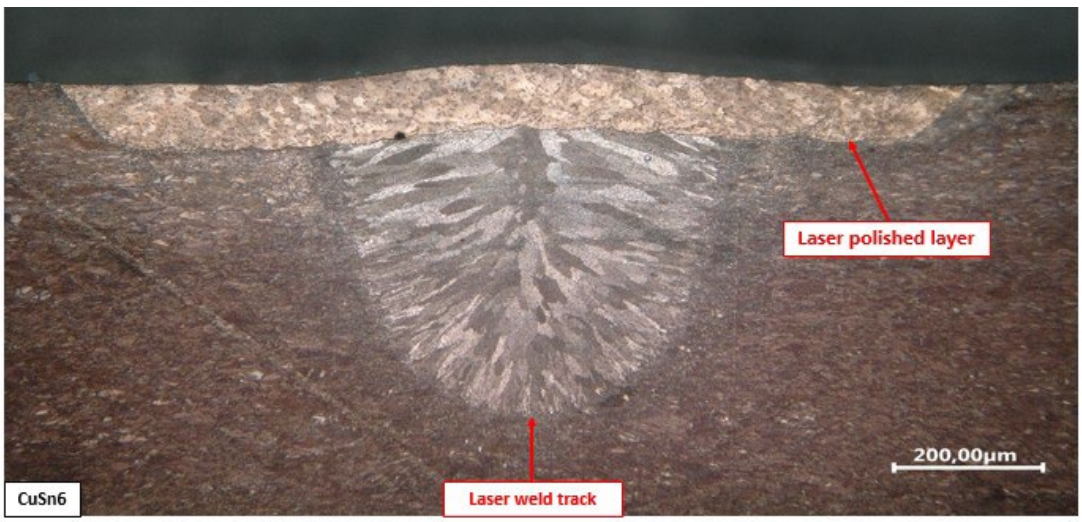

Fig. 8. Microscopic image of etched metallographic cross section of laser polished laser micro weld seam on CuSn6 using best parameters identified. The separate laser polishing tracks are clearly visible as well as the laser weld track which shows very strong contrast with large oriented crystal structure. The residual bulge of the weld track is also visible. Cracks or pores are not obvious in this sample.

The conclusion is similar to the results on Cu-ETP that simple scanning in X-direction, a medium scanning velocity of 100 mm/s and 2 passes together with laser powers close to evaporation limit are the favorable process parameters in this case. Again the largest possible melt pools have the additional advantage that melting as deep as possible potentially removes subsurface defects like pores.

Fig. 7. (a) and (b) shows a microscopic image of the best polishing result on CuSn6 and a false color height map calculated on the Keyence microscope of the same surface (polishing parameters P_L = 330 W, v_s = 100 mm/s, n = 2 passes yield a roughness of Ra = 4 ± 1 µm). In contrast to the relative flat (although fluctuating) weld track on Cu-ETP, the weld track on CuSn6 is bulged over the level of the initial surface. This could be caused by pores within the weld track, which effectively decrease the density and can lead to this bulging effect. As the cross section below does not show any signs of pores, this decrease in density is probably caused by a change in crystalline structure due to the rapid solidification. This needs to be investigated closer in future work. As can be seen, the laser polishing is able to significantly smoothen the ripples on the weld track surface and splatter on the sides. However the bulge of the weld track remains partially.

Fig. 8. displays the etched metallographic cross section of the laser polished laser micro weld track on CuSn6. The laser welding track is clearly visible with its large and oriented grain structure. The smaller laser polishing tracks are also clearly visible and show a different contrast and grain structure as the solidification is different in these smaller melt pools. The laser welding track reaches 535 ± 5 µm deep inside the CuSn6 while the laser polishing tracks start with a depth of 88 ± 2 µm which increases due to preheating to 105 ± 2 µm. These measured re-melting depths are significantly larger compared to Cu-ETP which coincides with the larger track widths and therefore larger melt pool sizes caused by the difference in heat conductivity. The laser polishing melts about one fifth as deep as the laser welding, which is a comparable ratio to the observed 6 to 1 on Cu-ETP.

5. Conclusion

The aim of this work is to identify a process window for laser polishing on laser weld seams on pure copper Cu-ETP and the copper alloy CuSn6 with green laser radiation. The first experiments on single tracks yield the physical limits of minimum and maximum laser power for stable melting for the two investigated laser beam diameters and show some technical limitations of the used laser source. Also the large difference in heat conductivity (5 times higher in pure copper over CuSn6) shows its influence on the process as Cu-ETP requires higher laser powers for melting and achieved lower maximum melt pool sizes compared to CuSn6. This growing process knowledge is further extended in experiments on areal laser polishing. Due to the preheating effect of previous melt tracks the process window shifts to lower laser powers which could not be fully investigated due to the high minimum laser power of the used Trumpf TruDisk Pulse 421 laser. Suitable parameters for area polishing are identified but the resulting roughnesses are larger or at best equal to the relative smooth initial state of the samples with Ra = 0.3 µm.

These results allow to further narrow down a suitable process window for polishing on weld seams which is investigated in the third step using only the larger laser beam diameter of 220 µm. Additionally to the previously varied process parameters laser power and scanning velocity, different scanning directions and multiple passes are investigated. It can be concluded that scanning velocity, direction of polishing and more than 2 passes have no significant influence on the achievable smoothening of the weld seams. In general higher laser powers close to the maximum possible power yield the best smoothening. On both materials the average roughness of the weld tracks could be lowered by a factor of 2 and maximum peaks and valleys were strongly reduced. The metallographic cross sections show no signs of pores or cracks before or after laser polishing and on both materials the welding track was five to six times deeper than the polishing tracks. All in all the objectives of this work could be achieved and laser polishing on laser weld seams on Cu-ETP and CuSn6 with green laser radiation is successfully demonstrated.

Acknowledgements

The presented investigations were carried out within the framework of the Collaborative Research Centre SFB1120 “Bauteilpräzision durch Beherrschung von Schmelze und Ersta rrung in Produktionsprozessen” and funded by the Deutsche Forschungsgemeinschaft e.V. (DFG). The sponsorship and support is gratefully acknowledged.

References

Hummel, M., Haeusler, A., Olowinsky, A., et al., 2020. Comparing 1070 nm and 515 nm Wavelength Laser Beam Sources in Terms of Efficiency for Laser Microwelding Copper, Lasers in Engineering 46, p. 187

Schmidt, P., 2015. Laserstrahlschweißen elektrischer Kontakte von Lithium-Ionen-Batterien in Elektro- und Hybridfahrzeugen, Dissertation. Technische Universität München, München.

Willenborg, E., 2006 Polieren von Werkzeugstählen mit Laserstrahlung, Dissertation RWTH Aachen, Shaker Verlag Aachen